



HAL
open science

Micro- and nanoplastics' transfer in freezing saltwater: Implications for their fate in polar waters

Alice Pradel, Maud Gautier, Dominique Bavay, Julien Gigault

► To cite this version:

Alice Pradel, Maud Gautier, Dominique Bavay, Julien Gigault. Micro- and nanoplastics' transfer in freezing saltwater: Implications for their fate in polar waters. *Environmental Science: Processes & Impacts*, 2021, 23 (11), pp.1759-1770. 10.1039/d1em00280e . insu-03341872

HAL Id: insu-03341872

<https://insu.hal.science/insu-03341872>

Submitted on 13 Sep 2021

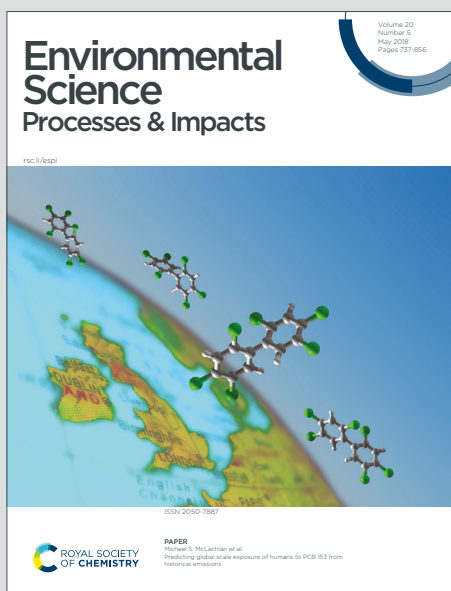
HAL is a multi-disciplinary open access archive for the deposit and dissemination of scientific research documents, whether they are published or not. The documents may come from teaching and research institutions in France or abroad, or from public or private research centers.

L'archive ouverte pluridisciplinaire **HAL**, est destinée au dépôt et à la diffusion de documents scientifiques de niveau recherche, publiés ou non, émanant des établissements d'enseignement et de recherche français ou étrangers, des laboratoires publics ou privés.

Environmental Science Processes & Impacts

Accepted Manuscript

This article can be cited before page numbers have been issued, to do this please use: A. Pradel, M. Gautier, D. Bavay and J. Gigault, *Environ. Sci.: Processes Impacts*, 2021, DOI: 10.1039/D1EM00280E.



This is an Accepted Manuscript, which has been through the Royal Society of Chemistry peer review process and has been accepted for publication.

Accepted Manuscripts are published online shortly after acceptance, before technical editing, formatting and proof reading. Using this free service, authors can make their results available to the community, in citable form, before we publish the edited article. We will replace this Accepted Manuscript with the edited and formatted Advance Article as soon as it is available.

You can find more information about Accepted Manuscripts in the [Information for Authors](#).

Please note that technical editing may introduce minor changes to the text and/or graphics, which may alter content. The journal's standard [Terms & Conditions](#) and the [Ethical guidelines](#) still apply. In no event shall the Royal Society of Chemistry be held responsible for any errors or omissions in this Accepted Manuscript or any consequences arising from the use of any information it contains.

Environmental Significance Statement

Accumulation of plastic debris in the Arctic Ocean has been predicted by ocean general circulation models and confirmed by field measurements. Understanding the behavior of plastic debris between seawater and ice is crucial to determine their distribution, transport, and accumulation in polar regions and to predict the potential impact of these particles on organisms and physical and biogeochemical processes. Our study proposes a new lab-scale experiment that reproduces sea-ice growth to evaluate the dynamic of microplastic vs. nanoplastics at the sea-ice interface. Our results demonstrate that while microplastics are retained in ice, nanoplastics are expelled from them, raising new questions about the possible localization, sink, and impact of plastic debris in the Arctic.

1
2
3
4
5
6
7
8
9
10
11
12
13
14
15
16
17
18
19
20
21
22
23
24
25
26
27
28
29
30
31
32
33
34
35
36
37
38
39
40
41
42
43
44
45
46
47
48
49
50
51
52
53
54
55
56
57
58
59
60

1
2
3
4
5
6
7
8
9
10
11
12
13
14
15
16
17
18
19
20
21
22
23
24
25

1
2
3
4
5
6
7
8
9
10
11
12
13
14
15
16
17
18
19
20
21
22
23
24
25

*Micro- and nanoplastics' transfer in freezing saltwater:
Implications for their fate in polar waters*

Pradel Alice^{1,2}, Gautier Maud¹, Bavay Dominique¹, Gigault Julien^{1,2}

¹ Univ Rennes, CNRS, Géosciences Rennes - UMR 6118, 35000 Rennes, France

² TAKUVIK, CNRS, Université Laval – UMI 3376, Quebec, Canada

Abstract:

Plastic debris accumulate in the Arctic by way of oceanic and atmospheric circulation. High concentrations of microplastics (1µm to 5 mm) have been measured, and nanoplastics (<1µm) are expected to be abundant as well. However, little is known about the mobility of micro- and nanoplastics at the seawater/ice interface. This study investigates the fate of micro- and nanoplastics during sea ice formation. A novel experimental approach simulates the growth of sea ice by progressively freezing a saline solution. After different durations of freezing, the concentration of NaCl, natural organic matter, microplastics, and nanoplastics was measured in the ice and liquid. Micro- and nanoplastics' distribution coefficient between saltwater and ice was determined, reflecting their behavior during congelation sea ice growth. The results show that microplastics are retained in ice while nanoplastics are expelled from it. Furthermore, natural organic matter plays a crucial role in stabilizing nanoplastics at this interface. These results raise new questions concerning the impact of micro- and nanoplastics in fragile polar environments and the analytical strategy to detect them.

Keywords:

Plastic debris, Arctic, Cryosphere, Pollution, Sea ice, Transfer, Natural Organic Matter

26 Introduction

27 Plastic debris is globally recognized as an urgent and multi-faceted issue(1–3). More than half
28 of all of the total plastic produced on Earth has been discarded(4) and due to mismanagement,
29 it is estimated that over 25% of all the plastic produced makes its way into the
30 environment(5). Microplastics (1µm to 5 mm) have already contaminated Earth's
31 compartments, from freshwater and terrestrial systems(6) to more remote areas such as the
32 Arctic Ocean(7–20). Indeed, microplastics were ubiquitous throughout Arctic waters and
33 sediments, with surface water concentrations ranging from 1.1×10^2 to 1.3×10^3 particles per
34 m^3 (14). Although comparing microplastic concentrations from different studies is difficult
35 due to the diversity of sampling and characterization methods, several studies suggest that
36 Arctic concentrations are close to those reported in populated areas and accumulation
37 zones(7,10–20). Indeed, average concentrations in surface waters of the Arctic Ocean of 0.34
38 ± 0.31 particles per m^3 are in the same order of magnitude than at the surface of the North
39 Pacific and North Atlantic subtropical gyres(7). Other studies found lower(10)
40 similar(11,12,12,16,17,19) or higher(14,16,18,19) surface and subsurface concentrations of
41 microplastics. Another study has concluded that while maximal concentrations are still higher
42 in subtropical gyres compared to the Arctic Ocean, median concentrations are similar(20). As
43 for other anthropogenic contaminants, long-distance transport of microplastic by atmospheric
44 and oceanic currents is responsible for their high concentration in the Arctic Ocean, where the
45 direct human impact is low(21,22). Indeed, Atlantic waters were identified as the primary
46 source of microplastics, followed by Siberian river waters(10). While analysis of fibers'
47 surface chemistry revealed that particles found in the western Arctic were increasingly
48 weathered, suggesting that inputs from the Atlantic Ocean or atmospheric deposition were
49 important sources(18). The number of microplastics in Arctic sediments are three orders of
50 magnitude higher than in surface and subsurface waters, corroborating that sediments are one
51 of the potential sinks of microplastics in the Arctic(14).

52 Sea ice is particularly impacted by microplastic contamination, since microplastics
53 accumulate in sea ice compared to seawater. Only one study simultaneously sampled
54 microplastics in both sea ice and the underlying seawater during the same expedition. In the
55 Arctic Central Basin, they found that the majority of microplastics detected were fibers and
56 their concentrations were approximately 3 orders of magnitude higher in sea ice than
57 seawater(19). Similar enrichment of microplastic in Antarctic sea ice was reported with
58 average concentrations of 3.1×10^{-2} particles per m^3 in surface water and 1.2×10^4 in sea
59 ice(23). Similarly, concentrations of microplastics in sea ice were significantly higher than in
60 accumulation zones such as the Pacific Gyre(8,9,15). When studying sea ice cores, snow, and
61 meltwater in the Western Arctic, the snow had a limited contribution to the overall sea ice
62 load of microplastics, suggesting instead that incorporation of microplastics dispersed in
63 seawater is the dominant pathway for accumulation in sea ice(15). After their accumulation in
64 sea ice, microplastics can be transported by sea ice drift and redistributed during sea ice
65 melt(9,19). Indeed, a thorough investigation of microplastic concentrations in polar waters
66 and sediments found that the highest concentration of their study (which was conducted
67 during one expedition, using the same sampling and analysis methods) was (1.3×10^3
68 particles per m^3) at the marginal ice zone in the surface waters of the Greenland Sea(14).
69 Therefore, it is crucial to better understand how plastic debris transfer between seawater and
70 sea ice, in order to determine their distribution, transport, and accumulation in polar regions.

1
2
3 71 This is especially critical since sea ice is a habitat that supports large communities of algae
4 72 which form the base of the food web(24,25). Furthermore, due to climate change, sea ice is
5 73 shifting from multi-year ice to thinner annual ice, making it especially important to
6 74 understand the mobility of plastic debris during sea ice growth(26).

7
8
9 75 While microplastics' presence in the Arctic and its impact on polar organisms have garnered
10 76 much attention(11,12,27,28), nanoplastics (< 1 μ m)(29) represent an invisible portion of
11 77 plastic debris unaccounted for in oceanic general circulation models(30,31) and impact
12 78 assessment(32,33). Indeed, during the lifecycle of plastic debris, photo-oxidative and
13 79 mechanical degradation produce nanoplastics(34–37). Due to their colloidal properties, such
14 80 as their high diffusivity and specific surface area, nanoplastics pose a potentially more
15 81 insidious risk compared to other sizes of plastic debris(38). Despite the scientific, political,
16 82 and public concern(1,33,39,40), to our knowledge, nanoplastics have not yet been detected in
17 83 the Arctic Ocean. This lack of evidence is due to their heterogeneous properties (size, shape,
18 84 composition, etc.) and the associated analytical challenges to characterize them in
19 85 environmental samples(29,41). However, nanoplastics are expected to be present due to the
20 86 long-range transport of plastic debris, allowing for more degradation. In particular, the ozone
21 87 depletion in polar regions is expected to accelerate plastic degradation into nanoplastics by
22 88 photo-oxidation(21,34,42).

23
24
25
26
27
28
29
30
31
32
33
34
35
36
37
38
39
40
41
42
43
44
45
46
47
48
49
50
51
52
53
54
55
56
57
58
59
60
89 Since quantifying microplastics and nanoplastics in polar environments is highly challenging
90 and since particles' mobility between seawater and ice is a complex process, experimental
91 modeling must be used to understand and predict the fate of these plastic debris(19). Indeed,
92 on top of analytical challenges, sampling microplastics and nanoplastics within sea ice and
93 polar waters presents additional challenges such as the variability of natural features (ice
94 structure, temperature, biological activity, etc.), seasonality, and lack of infrastructure.
95 Furthermore, the processes by which dissolved or particulate material is either rejected from
96 sea ice or captured in sea ice are complex(43,44). When water freezes, it rejects impurities
97 from its crystalline structure. A well-known example of this is the rejection of brine from sea
98 ice, which causes the sinking of cold and dense water, in turn driving the thermohaline
99 circulation(45,46). However, many of these dissolved species accumulate in localized areas of
100 the sea ice, which leads to the formation of bubbles (when gas' solubility limits are exceeded)
101 and brine pockets (as salts lower the freezing temperature of the liquid)(44,47). Different
102 processes lead to the accumulation of particulate species in sea ice. High enrichment of
103 particulate matter occurs during the growth of frazil ice in turbulent waters, which can lead to
104 the production of "dirty ice" enriched in sediments(48–50). Also, particles can be captured in
105 thick sea ice during congelation freezing in calmer waters. At this point, buoyant particles can
106 become entrapped in sea ice given a sufficient speed of advancement of the freezing
107 front(44,51–53). Globally, the capture of impurities in sea ice depends on parameters such as
108 particle size and density(48,51,54), the speed at which the freezing front
109 advances(52,53,55,56), water turbulence(49,50) as well as compatibility of the impurity with
110 solid water(51). In particular, for frazil ice growth, larger and denser sediments require more
111 turbulence to become suspended and entrapped in frazil ice crystals(48). For congelation
112 growth, larger particles can be entrapped at a lower speed of advancement of the freezing
113 front, compared to smaller particles(53,56). Since many processes co-occur, it is necessary to
114 understand how these separately affect the mobility of microplastics and nanoplastics.
115 Recently, a mesocosm experiment has studied the incorporation of microplastics during sea
116 ice growth(57). They found that microplastics were enriched in sea ice relative to the
117 underlying seawater. In particular, concentrations were highest at the surface, suggesting
118 efficient incorporation during initial sea ice formation and slower accumulation rates during

119 subsequent ice growth. However, to date, no experimental study has focused on nanoplastics
120 flux between seawater and ice.

121 This study aims to quantify microplastics and nanoplastics' flux between saltwater and a
122 freezing front in non-turbulent conditions. A novel lab-scale freezing reactor simulates the
123 seawater/ice interface and allowed the quantification of microplastic and nanoplastic transfer
124 between liquid water and a growing ice front. This freezing reactor has more controlled
125 freezing conditions than previous mesoscale studies(57), allowing for a more mechanistic
126 understanding of plastic particles' fate. Nanoplastics' stability at this interface was assessed in
127 light of their physical properties (size, surface, shape) and the presence of relevant natural
128 organic matter (NOM).

129 **Materials and Methods**

130 **Materials**

131 All solutions and colloidal dispersions were prepared with deionized (DI) water (Millipore,
132 18.2 MΩ). A stock solution of NaCl (solid, LabKem ExtraPure) was prepared at a
133 concentration of 100 g kg⁻¹. The sodium alginate (SA) stock solution was prepared by adding
134 SA (solid, Acros Organics) in DI water and agitating at 400 rpm for 12 hours. The stock
135 solutions had concentrations of approximately 1 g kg⁻¹ as determined with a Total Carbon
136 Analyzer (TOC-V CSH, Shimadzu, Japan). According to the SA's molecular composition, 1
137 mg kg⁻¹ of organic carbon was converted to 2.8 mg kg⁻¹ alginate.

138 The two spherical models studied, *nPSL-200* and *nPSL-350* were purchased from
139 Polysciences© (Polybead® Carboxylate Orange Dyed Microspheres 0.20 μm and Polybead®
140 Carboxylate Microspheres 0.35μm, Warrington USA). Stock dispersions at a concentration of
141 100 mg kg⁻¹ were prepared. The nanoplastic model with irregular shapes and polydisperse
142 sizes (*nPS-360*) was produced by mechanical abrasion of industrial-grade polystyrene (PS)
143 pellets (Total, Paris, France) with the method described by El Hadri et al. (2020)(37). Stock
144 solutions had a concentration of around 40 mg kg⁻¹. The PS pellets did not contain additives
145 and were not aged. The microplastic model (*μPS*) was obtained by grinding these same PS
146 pellets in a coffee grinder for 3 minutes, with interruptions to avoid overheating, and then
147 keeping the particles retained between sieves of 125 and 400 μm. In all experiments,
148 nanoplastic and microplastic concentrations were 10 mg kg⁻¹ and 4.25 g kg⁻¹, respectively.
149 These concentrations are higher than those expected in the environment(58), but were
150 necessary to remain within instruments' detection limits. All solutions' pH was fixed at 8
151 during 1 hour, using a pH-meter (F20, Mettler-Toledo, Schwerzenbach, Switzerland) and 0.1

1
2
3
4 152 mol kg⁻¹ solutions of NaOH (Fisher Scientific, Analytical Grade). A summary of stock
5 153 solutions' concentrations is provided in Supplementary Table 1. View Article Online
DOI: 10.1039/C4EM00280E

154 **Method**

155 The effect of freezing on the nanoplastic dispersions was studied in two setups: i) bulk
156 freezing and ii) partial and progressive freezing in a freezing reactor. For bulk freezing, glass
157 vials were filled with 3.5 mL of solution with varying concentrations of NaCl (5 to 55 g kg⁻¹)
158 and SA (1 to 100 mg kg⁻¹) and were either frozen at -22°C for 3 hours and thawed, or kept at
159 24°C. Each experimental condition was performed in triplicate. Bulk freezing was used to
160 study the effect of varying concentrations of NaCl and SA on the stability of nanoplastics.
161 Nanoplastic' colloidal stability was assessed by measuring changes in size and concentration
162 between the nanoplastic dispersions that underwent a cycle of freeze/thaw and those that
163 remained at room temperature. For the partial and progressive freezing experiments, the
164 experimental protocol is thoroughly illustrated in Supplementary Figure 1. Briefly, 12 mL of
165 solution was inserted in a vessel, which had a capacity of 22 mL. At the end of the
166 experiment, the part of the solution that remained liquid was recovered, then the bottom of the
167 vessel was then rinsed, and finally, the thawed ice was recovered. Once the solutions returned
168 to room temperature, the mass of each phase was weighed, and the solutions were
169 characterized by measuring pH, the concentration of NaCl, micro- and nanoplastics and SA,
170 and the size of nanoplastics. The freezing reactors' vessel and the cold finger were composed
171 of glass with thicknesses between 1.8 and 2 mm. The cold finger contains a cooling liquid in
172 constant circulation through a thermostat (Ecoline RE106 Lauda, Delran, USA). Two reactors
173 were set up in parallel to obtain duplicate experiments.

174 The internal temperature of the cold finger was $-6.7 \pm 0.6^\circ\text{C}$. Ice formation was described by
175 time-lapse photography (Supplementary Figure 2). The first ice was observed after 7 minutes
176 in DI water and after 9 minutes in 35 g kg⁻¹ NaCl. The maximum freezing speed was 8 $\mu\text{m s}^{-1}$
177 in DI and 4 $\mu\text{m s}^{-1}$ in NaCl. In DI, the ice grows first parallel to the sides of the refrigerating
178 piece. Upon attaining the walls of the vessel (at 20 to 25 minutes), the ice then grows
179 vertically and stabilizes after 3 hours. In NaCl, freezing follows the same dynamic, except the
180 ice (i) has a more rounded shape, (ii) reaches the walls of the vessel after 25 to 30 minutes,
181 and finally, (iii) the underneath of the ice, in contact with the liquid, systematically thaws
182 after approximately 1.5 hours, after which the ice volume stabilizes. The volume of ice
183 formed in DI is 35% superior to that formed in NaCl.

184 The z-average hydrodynamic diameters (d_{zH}) were determined by a dynamic light scattering
185 (DLS) probe (Vasco-Flex, Cordouan Technologies, Pessac, France). The backscattered light
186 is collected at a geometric angle of 170° with respect to the incident beam direction. Each
187 measurement was obtained from an average of five correlation functions that were
188 accumulated for 60 seconds. d_{zH} is obtained by fitting a monomodal, normal distribution to
189 the raw data (Cumulant algorithm ISO 22412:2008). Nanoplastic concentrations were
190 measured by absorption at a wavelength of 226 nm (UV-2600UV-Visible Spectrophotometer,
191 Shimadzu, Japan). Alginate concentrations were measured by Total Carbon Analyzer (TOC-V
192 CSH, Shimadzu, Japan). The ionic strengths and pHs were measured with a conductivity
193 meter and pH meter (F30 and F20, Mettler-Toledo, Schwerzenbach, Switzerland). The surface
194 potential of the nanoplastics was assessed using a Wallis zetameter (Cordouan Technologies,

1
2
3 195 Pessac, France). The zetameter measures the electrophoretic mobility by laser Doppler
4 196 electrophoresis and applies the Smoluchowski model to determine the zeta potential. Mass
5 197 balances were calculated with the mass of initial solution (M_{Init}), and liquid (M_{Liq}) and ice
6 198 (M_{Ice}) solutions recovered from the freezing reactor, as well as the SA or particle
7 199 concentrations measured in the initial solution (C_{Init}), and in the liquid (C_{Liq}) and ice (C_{Ice})
8 200 solutions recovered from the freezing reactor. Mass balance of liquid lost was calculated as:

$$\frac{M_{Init} - (M_{Liq} + M_{Ice})}{M_{Init}}$$

11 201
12
13
14 202 A positive (negative) value indicates a loss (gain) of mass. The distribution of initial SA or
15 203 particle masses between liquid and ice were calculated as:

$$\frac{(C_{Liq} * M_{Liq})}{(C_{Init} * M_{Init})}$$

17 204
18
19 205 for the liquid phase, and as:

$$\frac{C_{Ice} * M_{Ice}}{C_{Init} * M_{Init}}$$

20 206
21
22 207 for the solid phases. Losses of SA or particle masses were calculated as 1- (Proportion in
23 208 Liquid + Ice). Percent variations in concentration (C) and sizes (d_{zH}) were given by the
24 209 following equations:

$$\frac{(C_{final} - C_{initial})}{C_{initial}} * 100$$

25 210
26 211 and

$$\frac{(d_{zH\ final} - d_{zH\ initial})}{d_{zH\ initial}} * 100$$

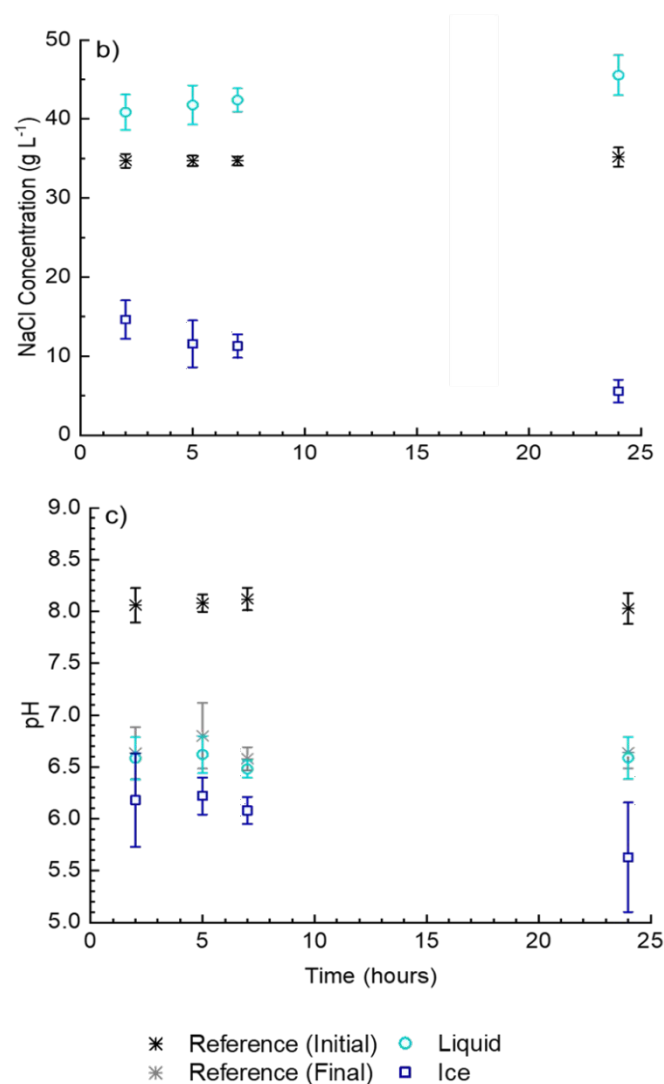
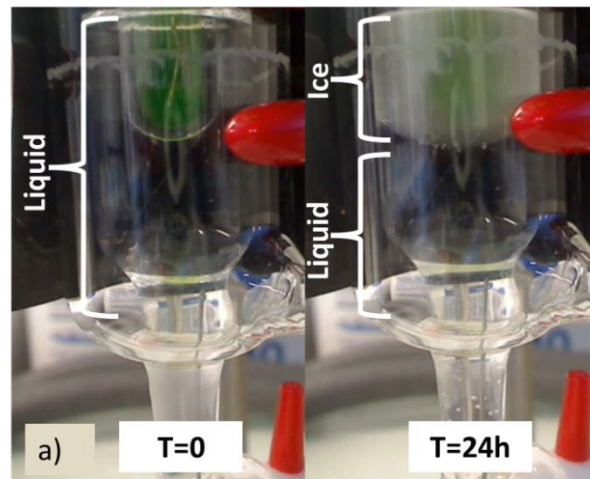
23 212 24 213 **Results and Discussion**

25 214 Freezing reactors were designed to partially and progressively freeze aqueous solutions,
26 215 simulating growing sea ice (Figure 1a and Supplementary Figures 1, 2 and 3a). These were
27 216 composed of vessels containing a solution of 35 g kg⁻¹ NaCl at pH 8 and a cold finger that
28 217 was inserted in the solution (t=0). The evolution of the ice and liquid's physical and chemical
29 218 properties (water mass, ionic strength, and pH) were investigated (Figures 1b and 1c and
30 219 Supplementary Figure 3b). The water mass balance (the difference between the initial water
31 220 mass and the sum of liquid and ice masses recovered) is generally well conserved. Indeed, as
32 221 can be seen in Supplementary Table 2, throughout the 64 data points, most had a final mass
33 222 balance within $\pm 6\%$ of the initial mass. 78% of data points have a positive mass balance
34 223 indicating a loss of mass. This can be explained by liquid retained on the surfaces of the
35 224 freezing reactor vessel and in the faucet by capillary action. On the other hand, gain of mass
36 225 can be explained by condensation of water vapor in the air due to the cold temperatures
37 226 (either during the experiment or when recovering liquid and ice). Only on 6 occasions, the

227 mass balance was superior to $\pm 6\%$, with a loss of 7%, 7%, 8%, and 22% and two gains of
228 18%. View Article Online
DOI: 10.1039/D1EM00280E

229 The initial NaCl concentration is 35 g kg^{-1} which is typical of the Atlantic sector of the Arctic
230 Ocean and areas below 80° N (59). During freezing, NaCl segregates between liquid and ice:
231 its concentration decreases in ice and increases proportionally in the liquid phase, reaching 40
232 g kg^{-1} (Figure 1b). This is due to freeze-exclusion, the mechanism by which impurities such as
233 ions are expelled from the crystalline structure of ice. Some of the NaCl is not expelled out of
234 the ice structure but is incorporated in it, forming the brine channels and pockets(55,60).
235 These zones remain liquid since the accumulation of salt lowers the freezing point of brine.
236 Hence, in ice, substantial heterogeneity in NaCl concentrations is expected. Nonetheless, the
237 average salinity of ice decreases from 14.6 g kg^{-1} at 2 hours, which is typical of the early
238 stages of freezing(60,61) to 5.6 g kg^{-1} at 24 hours, which is typical for first year ice(46,62).
239 The mass balance of salts was also generally conserved. Although the amount of NaCl losses
240 ($7.6 \pm 3.3 \%$) was superior to the mass of water losses ($2.0 \pm 5.6 \%$) it was less variable. There
241 is only a slight positive correlation between mass of water lost and mass of NaCl lost ($R^2 =$
242 0.19). There is no correlation between mass of particles or alginate lost and mass of NaCl lost
243 ($R^2 = 0.08$) (Supplementary Table 2). The loss of NaCl cannot be attributed to precipitation
244 since NaCl is soluble at these temperature and concentrations. However, since conductivity is
245 positively correlated to temperature, this loss of NaCl could be a deviation caused by
246 measurements of conductivity at temperatures slightly lower than the ambient temperature,
247 despite the care in waiting for samples to return to ambient temperature.

248 Freezing is known to produce changes in pH(61,63) and nanoplastics are sensitive to pH
249 changes when they contain surface functional groups such as carboxylic acids (which is the
250 case for *nPSL-200* and *nPSL-350*)(5). Therefore, the pH changes during freezing were
251 investigated. Initially, the pH of all solutions studied are fixed at 8.07 ± 0.05 , as illustrated by
252 “Reference (Initial)” in Figure 1c. During the experiment, a part of this initial solution is kept
253 at room temperature and shows a decrease in pH of 1.42 ± 0.12 pH units, as illustrated by
254 “Reference (final)” (Figure 1c). This is due to the reaction of atmospheric CO_2 with hydroxide
255 ions which forms carbonates. The pH of the liquid and thawed ice recovered from the freezing
256 reactors, were measured at room temperature. In the liquid phase, the decrease in pH is not
257 significantly different from that of the same solution kept at room temperature (-1.50 ± 0.29
258 pH units). However, the thawed ice is systematically more acidified: with a decrease of $2.04 \pm$
259 0.25 pH units. This is due to the higher solubility of CO_2 at lower temperatures, which
260 increases the transfer of aqueous CO_2 to the colder section of liquid in the freezing reactor.
261 This is supported by the fact that there is no enhanced acidification after complete (bulk)
262 freeze/thaw experiments, compared to a solution that remained at room temperature. This
263 evolution of pH typical of that of sea ice without photosynthetic activity, since in natural sea
264 ice, the excess CO_2 in ice is consumed by photosynthetic organisms(61).



265

266 *Figure 1 : a) Freezing reactor at the beginning of freezing (T=0) and after 24 hours of freezing (T=24h) of 35 g*
 267 *kg⁻¹ NaCl. Evolution of (b) NaCl concentrations and (c) pH of the liquid, thawed ice, and reference solution, for*
 268 *initial solutions containing 35 g kg⁻¹ NaCl at pH 8 frozen in the freezing reactor. (n=40, i.e.: duplicates of 20*
 269 *different solutions; whiskers represent standard deviation).*

270 Model nanoplastics and microplastics were used to study the segregation of these particles at
 271 a growing freezing front. Their properties are summarized in Table 1 and images are
 272 presented in Supplementary Figure 4. Concerning nanoplastics, two spherical polystyrene
 273 latex (PSL) particles with monodisperse sizes of 200 nm (*nPSL-200*) and 350 nm (*nPSL-350*)
 274 and a more environmentally relevant nanoplastic model (*nPS-360*) were studied. *nPSL-200*
 275 contain trace amounts of surfactants whereas *nPSL-350* have been purified. Finally, *nPS-360*
 276 is produced by mechanical abrasion of polystyrene (PS) pellets. Due to the synthesis method,
 277 *nPS-360* are surfactant-free and have an irregular, asymmetrical shape and polydisperse sizes.
 278 Nanoplastics' behavior was assessed in the presence of sodium alginate (SA). SA is a natural
 279 organic matter (NOM) that serves as a proxy for exopolymeric substances (EPS)(64) which
 280 are abundant in sea ice(65). The surface potential showed that *nPSL-200* and *nPSL-350*, with
 281 zeta-potentials of -50.5 ± 5.5 mV and -43.7 ± 5.1 mV, respectively, are more negatively
 282 charged than *nPS-360*, which has a zeta-potential of -28.1 ± 5.6 mV. This also contributes to
 283 making *nPS-360* a more environmentally relevant particle. The presence of SA did not
 284 significantly modify the surface potential of nanoplastics (Supplementary Figure 5). Finally, a
 285 microplastic model (μ PS) was produced using the same PS pellets as for *nPS-360*.

286 *Table 1: Characteristics of the nanoplastic (nP) and microplastic (μ P) models studied.*

| Name | Synthesis Method | d_{zH}^a or Sieve Mesh Size* (μ m) | PDI ^b | Morphology | Natural Organic Matter | Environmental Relevance |
|----------------------|--|---|------------------|----------------------------|------------------------|-------------------------|
| <i>nPSL-200</i> | Emulsion polymerization | 0.168 | 0.0261 | Spherical | No | - |
| <i>nPSL-200</i> + SA | | | | | Alginate | + |
| <i>nPSL-350</i> + SA | Emulsion polymerization Surfactant-free | 0.337 | 0.0889 | | Alginate | ++ |
| <i>nPS-360</i> + SA | Mechanical abrasion of PS pellets | 0.364 | 0.102 | Asymmetrical and irregular | | +++ |
| μ PS | | 125 to 400 * | NA | Asymmetrical and irregular | No | ++ |

287 ^az-average hydrodynamic diameter; ^bPolydispersity index (PDI), defined as the variance of the Gaussian-fitted
 288 size distribution.

289 Nanoplastics are sensitive to concentrations of NaCl and SA due to their colloidal properties.
 290 Indeed, on the one hand, NaCl may cause rapid aggregation and sedimentation by screening
 291 the electrostatic repulsion between particles. On the other hand, SA prevents this
 292 destabilization by electrostatic and steric repulsion(66). The ice growth in the freezing reactor
 293 produces gradients of NaCl and SA (the latter will be discussed below). Therefore,
 294 nanoplastics' stability after freeze/thaw was assessed with varying concentrations of SA and
 295 NaCl: in addition to the experiments conducted in the freezing reactor, nanoplastics' were
 296 studied in bulk experiments by entirely freezing solutions at -20°C and thawing them at 24°C .

297 After bulk freeze/thaw *nPSL-200* formed aggregates independently of NaCl and SA
 298 concentrations (Supplementary Figure 6). As solidifying water rejects particles from its
 299 crystalline structure, their concentration increases at the freezing front, which increases the
 300 possibility of collision and induces aggregation(67). Indeed, freezing is known to destabilize
 301 colloidal dispersions such as biopolymers (ex: milk) and solid colloids (ex: latex paints,

nanoplastics)(67–69). In pure water (without NaCl), the aggregation is more likely due to the strong mechanical stress caused by the growth of the homogenous crystalline structure of ice(70). However, with NaCl, the ice structure is more porous, causing less mechanical stress. In this case locally high concentrations of NaCl are more likely to cause aggregation. When *nPSL-200* are frozen in NaCl without SA, the large aggregates sediment, causing a 22 to 41% decrease in concentrations compared to particles that remained at room temperature (Figure 2a). However, with 50 mg kg⁻¹ SA the aggregates formed did not sediment (Figure 2a). SA also successfully stabilized *nPSL-350* and *nPS-360* after one freeze/thaw cycle with up to 55 g kg⁻¹ NaCl (Figure 2a). At 35 g kg⁻¹ NaCl, even low concentrations of SA (15 mg kg⁻¹) are sufficient to stabilize all particles (Figure 2b). This demonstrates that the association of SA with nanoplastics prevents their destabilization during freezing. Since naturally occurring organic matter is expected to be more abundant than nanoplastics(58,71) and to study nanoplastics that retained their colloidal behavior during freezing, the initial concentration of SA in the freezing reactor was set at 50 mg kg⁻¹ (for an initial concentration of nanoplastics of 10 mg kg⁻¹).

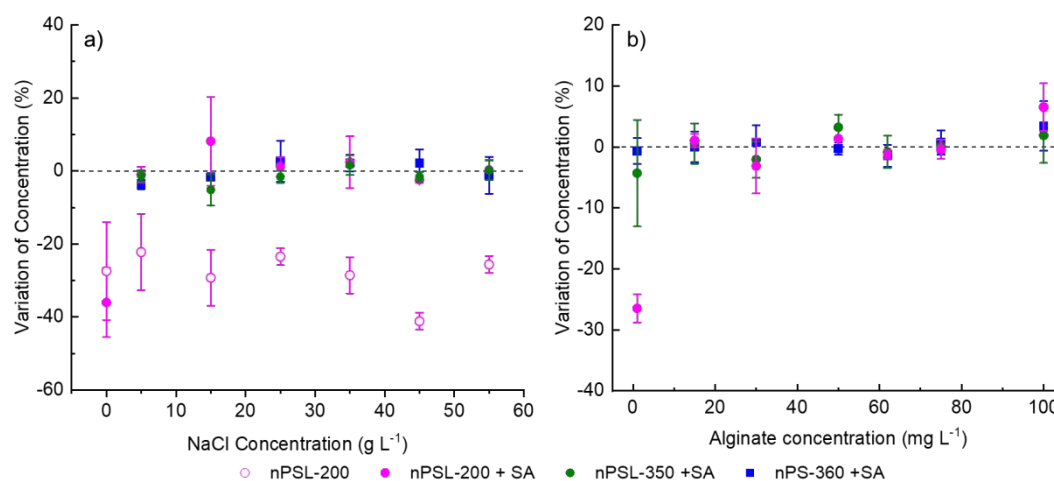
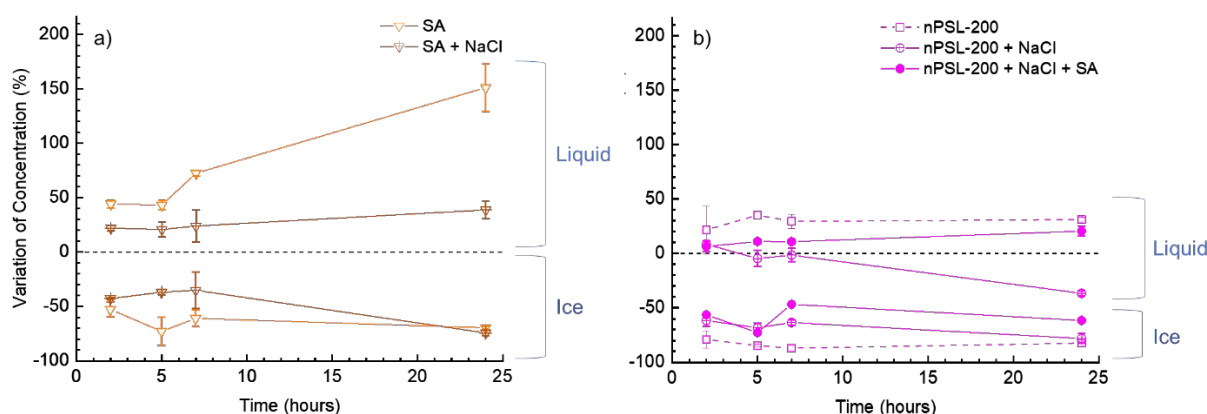


Figure 2: Variations of concentration of nanoplastics (nPs) after bulk freeze/thaw a) as a function of NaCl concentration (keeping SA at 50 mg kg⁻¹, if present) and b) as a function SA (keeping NaCl at 35 g kg⁻¹ NaCl).

When solutions are frozen in the freezing reactor, nanoplastics and SA can separate between liquid and solid phases, mimicking their mobility during sea ice growth in polar waters. Figure 3 shows the relative distribution of SA (Figure 3a) and *nPSL-200* (Figure 3b) between water and ice, in de-ionized water and in 35 g kg⁻¹ NaCl. All concentrations of species that were frozen in the reactor are presented in Supplementary Table 2. Both species are expelled from ice to water, akin to NaCl. For both SA and *nPSL-200*, the expulsion from ice to water is less pronounced when NaCl is involved (Figure 2 and Supplementary Figure 7). As for bulk experiments, in the freezing reactor losses of SA and *nPSL-200* mass are higher in deionized water (12 ± 10% for SA and 30 ± 7% for *nPSL-200*) than in 35 g kg⁻¹ NaCl (-1 ± 4% for SA and 27 ± 16% for *nPSL-200*). The growth of pure water crystals without the porous areas formed by brine physically forces alginate molecules and *nPSL-200* particles together(68,70). When frozen in NaCl, they are subject to less shear strength in the brine pockets than between the pure ice crystals of deionized water. Therefore, SA and *nPSL-200* frozen in deionized water aggregate and either are not recovered from the faucet of the freezing reactor or, if recovered, sediment out of solution due to their large size. In both cases, this fraction will not be measured by absorbance or total organic carbon measurements, which leads to losses in the mass balance. The loss of SA and *nPSL-200* when frozen in deionized water as well as the increased proportion of SA and *nPSL-200* present in ice when frozen in 35 g kg⁻¹ NaCl

338 strongly suggests that SA and *nPSL-200* are trapped in brine pockets. Indeed, the
 339 accumulation of NOM in brine pockets has already been established(43,72). View Article Online
DOI: 10.1039/D1EM00280E

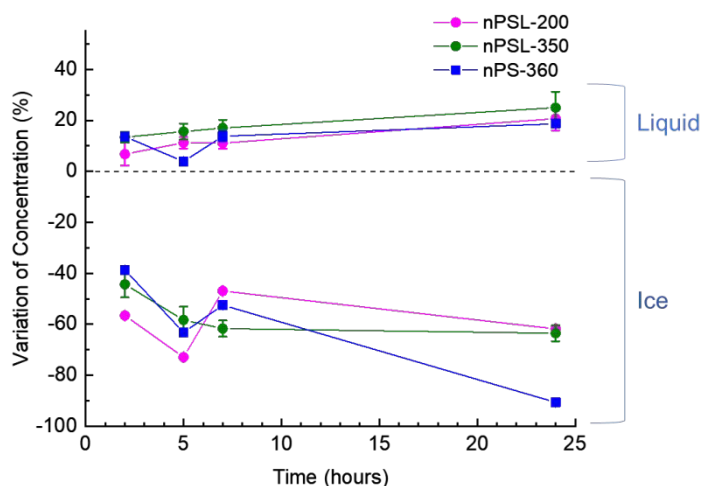
340 When *nPSL-200* is dispersed in NaCl without SA, their concentration decreases in both liquid
 341 and ice, indicating a global loss of mass (Figure 3b). Indeed, losses amount to $10 \pm 2\%$, $29 \pm$
 342 5% , $24 \pm 0\%$, $52 \pm 3\%$ of the total mass at 2, 5, 7 and 24 hours (Supplementary Table 2). This
 343 is due to aggregation followed by sedimentation in the liquid, as predicted by bulk
 344 experiments (Figure 2a), and confirmed by size measurements (discussed below). Globally,
 345 SA's presence significantly reduced the loss of nanoplastics by sedimentation in 35 g kg^{-1}
 346 NaCl with losses equal to $9 \pm 7\%$, $6 \pm 2\%$, $7 \pm 7\%$, $13 \pm 7\%$ of total mass at 2, 5, 7 and 24
 347 hours (Supplementary Table 2). These losses show no time-dependency which confirms that
 348 SA has a stabilizing role, since aggregation is time-dependent. Similarly, losses of *nPSL-350*
 349 and *nPS-360* in NaCl and SA did not show time-dependency and were of the same magnitude
 350 ($11 \pm 3\%$ and $8 \pm 3\%$ averaged over the four freezing durations, for *nPSL-350* and *nPS-360*
 351 respectively).



352
 353 *Figure 3 : Variation of the concentration of a) SA and b) nPSL-200 in liquid and ice, as a function of the*
 354 *duration of freezing in the reactor. The empty symbols represent de-ionized water at pH 8. Symbols with a cross*
 355 *represent 35 g kg^{-1} NaCl at pH 8. For nPSL-200, the full symbol represents a dispersion in 35 g kg^{-1} NaCl and*
 356 *50 mg kg^{-1} SA at pH 8.*

357 All nanoplastic models (*nPSL-200*, *nPSL-350*, and *nPS-360*) show the same global behavior
 358 in the presence of NaCl and SA (Figure 4). Their concentration increases in the liquid and
 359 decreases in the ice over time, following a similar trend as that of NaCl and SA
 360 (Supplementary Figure 8). In ice, *nPSL-200* concentration is reduced by 47 to 53%, while the
 361 concentrations of *nPSL-350* and *nPS-360* decrease continually (-45% to -63% and -38% to -
 362 90%, respectively). The larger *nPSL-350* is more slowly expelled from ice than its smaller
 363 counterparts (*nPSL-200* and *nPS-360*). Indeed, most *nPS-360* particles are smaller than their
 364 hydrodynamic diameter ($d_{zH} = 360 \text{ nm}$), since due to the high polydispersity of the size
 365 distribution (PDI = 0.102) the scattered light is dominated by the larger particles(73,74). The
 366 diffusion coefficient drives the rate of expulsion from ice to saltwater, as expected
 367 theoretically(75,76). Indeed NaCl, which diffuses most rapidly, has a stronger expulsion rate
 368 (Supplementary Figure 8). However, SA is slowly expelled from ice due to its linear structure
 369 which prevents it from diffusing like salts or colloids (Figure 2 and Supplementary Figure 8)

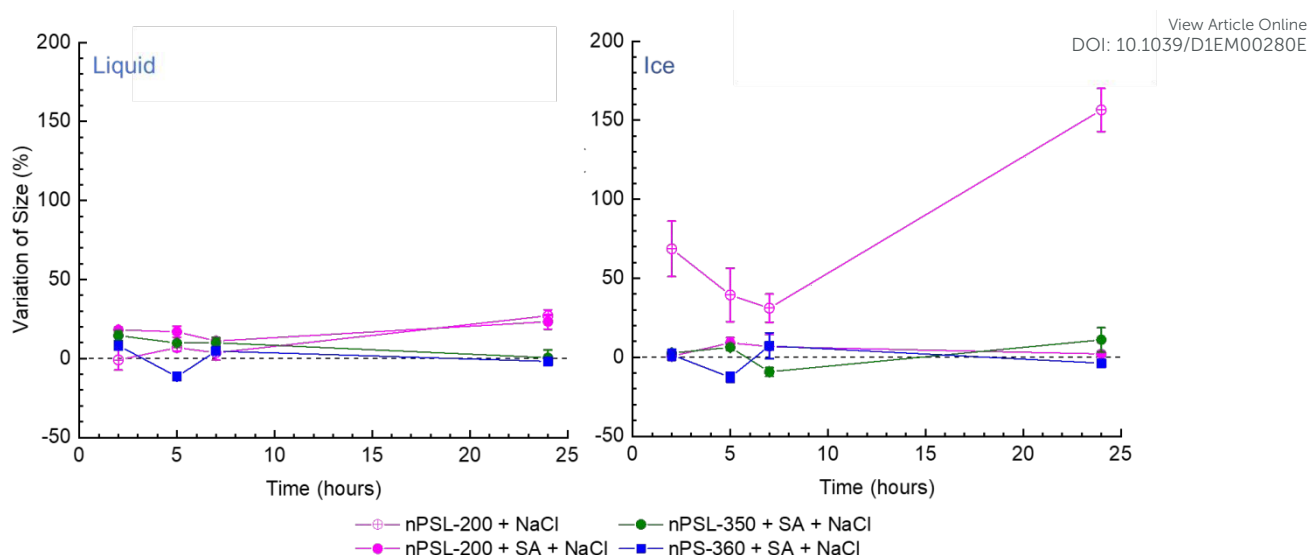
370 (43,65). Even though *nPS-360* has many particles that are similar in size to *nPSL-200*, they
 371 are not expelled from the ice at the same rate. Since particles are likely to aggregate in ice and
 372 since nanoplastics are particularly sensitive to aggregation, differences in nanoplastic
 373 retention in ice during freezing could be attributed to differences in aggregation states.



374
 375 *Figure 4: Variation of the concentration of nanoplastics (nPs) in the liquid and ice, as a function of the duration*
 376 *of the freezing in the reactor. Nanoplastics were dispersed in 35 g kg⁻¹ NaCl and 50 mg kg⁻¹ SA at pH 8.*

377 To understand differences in nanoplastic retention in ice, variations of nanoplastics' sizes
 378 recovered in liquid and ice were investigated (Figure 5). With NaCl and SA no aggregation is
 379 observed, and all nanoplastics (*nPSL-200*, *nPSL-350* and *nPS-360*) remain stable in both
 380 saltwater and ice. SA stabilizes nanoplastics at high ionic strength by wrapping the particles
 381 and providing electrostatic and steric repulsion between the particles(66). So, the differences
 382 in expulsion between different types of nanoplastic cannot be attributed to differences in
 383 aggregation state. Without SA, *nPSL-200* that remained in ice are aggregated, whereas they
 384 are not in the liquid. In the liquid, aggregated *nPSL-200* can sediment and leave the
 385 suspension during the experiment, as illustrated by the significant losses of *nPSL-200* in these
 386 conditions (Supplementary Table 2). However, in ice, *nPSL-200* are trapped at high
 387 concentrations in brine pockets and channels. They aggregate due to higher collision rates and
 388 favorable collisions (screened the electrostatic repulsion), as observed in bulk freezing
 389 experiments and cannot sediment out of the ice (Supplementary Figure 6).

390



391

392 *Figure 5: Variation of the hydrodynamic radius (d_{H}) of different nanoplastic particles dispersed in 35 g kg⁻¹*
 393 *NaCl and recovered from liquid (left) and ice (right) after different durations of freezing in the reactor.*

394 Due to their larger size and buoyancy, microplastics' showed an opposite behavior compared
 395 to nanoplastics (Supplementary Figure 9). The proportion of microplastics located in the ice
 396 was $68 \pm 10\%$ after 2 hours of freezing, $76 \pm 9\%$ after 5 hours, $69 \pm 10\%$ after 7 hours and 77
 397 $\pm 4\%$ after 24 hours. Total losses of microplastics are not time-dependent and were generally
 398 higher and more variable than for nanoplastics ($14 \pm 8\%$ and $9 \pm 4\%$ for microplastics and
 399 nanoplastics, respectively, Supplementary Table 2). Contrary to nanoplastics or others
 400 colloidal materials, microplastics are not a homogenous dispersion. Therefore, small losses of
 401 water mass can lead to large losses of microplastic particles. Also, due to their larger size, it is
 402 more likely that microplastics be retained in the vessel.

403

404 Microplastics' incorporation in ice depends on their location at the moment of freezing. Since
 405 all microplastic particles studied here are buoyant, they were preferentially entrapped in the
 406 ice which grows from top to bottom. Since the volume of microplastics in ice are much higher
 407 than volume of brine pockets and channels it is expected that these particles are not solely
 408 trapped in brine pockets and channels (as are nanoplastics), but rather entrapped by the
 409 growing ice crystals. Microplastics' buoyancy is attributed to their density and to their
 410 hydrophobicity. Microplastics' density of 1055 kg em^{-3} is relatively close to that of 35 g kg^{-1}
 411 NaCl (1020 kg m^{-3}). Also, microplastics were hydrophobic since they were produced from
 412 pure PS which was mechanically degraded but not oxidized. Due to their hydrophobicity, a
 413 large part is attracted to the air/water interface due to the surface tension of water(77), similar
 414 to accumulation of microplastic at sea surface microlayer(78). Mesocosm experiments also

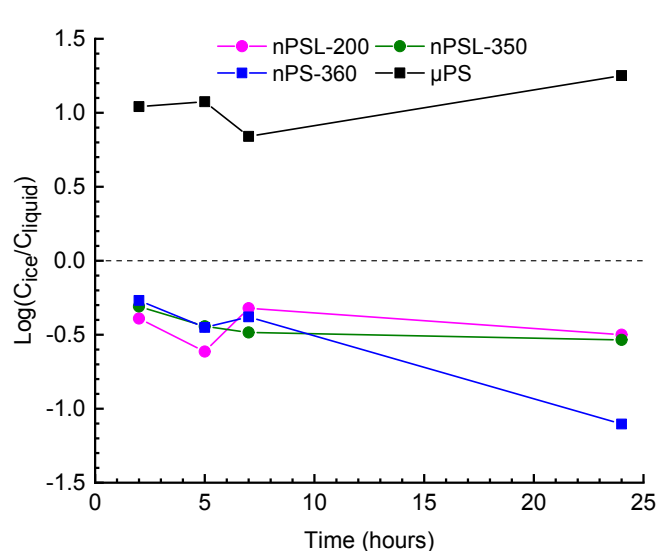
415 showed that during the initial stages of freezing, ice crystals preferentially trap low density
416 microplastics(57).

417
418 The use of initial microplastic mass concentrations that are higher than nanoplastic
419 concentrations could lead to differences in the morphology and speed of the freezing front,
420 and therefore to their microplastics' distribution between liquid and ice(75,79). However, we
421 observed no differences in the speed of advancement of the freezing front, in the proportion of
422 liquid and ice formed, nor in the distribution of NaCl between liquid and ice. High particle
423 concentrations can also lead to entrapped of multiple particles at a time which could lead to
424 higher enrichment rate in ice(79). However, this is a minor effect compared to the importance
425 of the speed and morphology of the freezing front(79). Therefore, our conclusions about
426 nanoplastics and microplastics behavior in saltwater remain valid despite our use of
427 concentrations that are significantly higher than concentrations measured or estimated in the
428 environment(58).

429
430 Due to their large size, microplastics movement is solely affected by gravity and water
431 advection. In this experimental setup, there is only water convection caused by differences in
432 salinity and temperature, which is minimal compared to the water flow expected in the Arctic
433 Ocean. So, while we show that micrometric fragments of PS will be trapped by ice if they are
434 in the vicinity of the ice front, processes are expected to be more complex in the environment.
435 First of all, water turbulence can move microplastics into the sea ice matrix, comparable to
436 microplastic transport in porous media. Secondly, differences in behavior can be expected
437 depending on microplastic composition and shape. Microplastics in polar waters have a wide
438 array of compositions (polyethylene, polyethylene terephthalate, etc) and some studies
439 suggest that the majority are fibers(8,15,17–19). Finally, microplastics in the Arctic Ocean are
440 mostly expected to come from distant areas. Therefore, their surface is expected to be highly
441 oxidized and covered with an eco-corona. Due to this surface aging, they may be less
442 hydrophobic and have less affinity for the air/water interface.

443
444 Based on this experimental work, we propose, for the first time, a distribution coefficient of
445 nanoplastics and microplastics between the ice and the saltwater $\log(\frac{C_{ice}}{C_{liquid}})$, illustrated in
446 Figure 6 according to the freezing time. This experimental work shows that plastic debris
447 have size-dependent behavior at this saltwater/ice interface. This is expected from previous
448 experiments and field studies concerned with the distribution of natural particles between
449 saltwater and ice(43,51,56,75,76,79). Indeed, the distribution coefficient is negative for
450 nanoplastics (ranging from -0.27 to -1.10) and positive for microplastic (0.85 to 1.26). For
451 both the microplastics and nanoplastics, except *nPS-360*, no clear evolution of the distribution
452 coefficient is observed over time, showing the importance of the first stage of ice formation
453 on the segregations of plastic debris according to their size. The continued expulsion of *nPS-*
454 *360* in ice at 24 hours, should be further explored. These distribution coefficients can be
455 inform numerical models of plastic debris' fate in the Arctic(80).

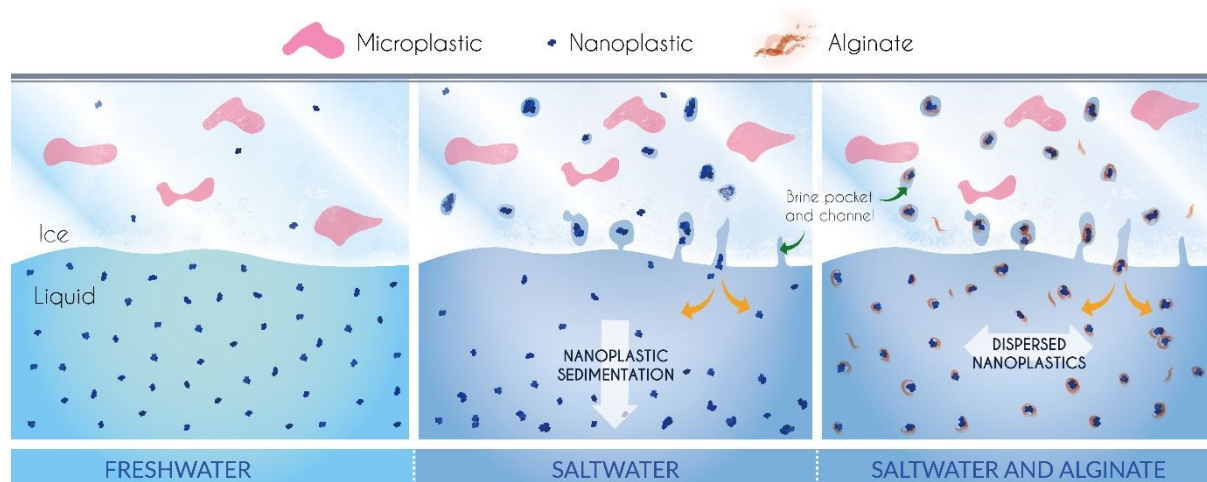
456



View Article Online
DOI: 10.1039/D1EM00280E

457
458 *Figure 6: Logarithm of nanoplastics' and microplastics' distribution between ice and liquid phase (C_{ice}/C_{liquid}) as*
459 *a function of the duration of freezing in the freezing reactor. Experiments were conducted with $35 \text{ g kg}^{-1} \text{ NaCl}$*
460 *and $50 \text{ mg kg}^{-1} \text{ SA}$.*

461 The different behaviors of micro- and nanoplastics expected during congelation growth of sea
462 ice are summarized in Figure 7. Due to their colloidal nature, most nanoplastics are rapidly
463 expelled from sea ice, whether formed from freshwater (left) or saltwater (middle and right).
464 The nanoplastics retained in freshwater ice may be strongly aggregated by the shear stress of
465 growing ice crystals (aggregates not shown). Nanoplastics frozen in saltwater will be able to
466 accumulate in the brine pockets of sea ice. The growing ice front entraps non-colloidal
467 plastics (microplastics). In saltwater, SA stabilized nanoplastics during freezing (right),
468 suggesting that native NOM with high polysaccharide content will cause nanoplastics to
469 remain suspended under sea ice. However, this saltwater/ice interface is also rich in sinking
470 materials of chemical and biological origin such as gypsum and algae, which will propel
471 nanoplastics down the water column to sediments(25,61). So, while sea ice acts as a medium
472 to short-term sink for microplastics, it may accelerate nanoplastics' sedimentation. This
473 highlights the fact that sub-micrometric plastic debris cannot be lumped into the same
474 category as microplastics(29).
475



476
477 *Figure 7: Summary of nanoplastics' and microplastics' behaviors at the water/ice interface as a function of*
478 *water composition*

479
480 **Author Contributions:** Pradel Alice: Formal Analysis, Investigation, Methodology,
481 Supervision, Writing – original draft, Writing – review & editing; Gautier Maud:
482 Investigation, Methodology; Bavay Dominique: Investigation, Resources; Gigault Julien:
483 Conceptualization, Supervision, Funding acquisition, Writing – original draft, Writing –
484 review & editing.

485 **Conflict of Interest:** There are no conflicts to declare.

486 References:

- 487 1. SAPEA, Science Advice for Policy by European Academies. A Scientific Perspective on
488 Microplastics in Nature and Society [Internet]. Berlin: SAPEA; 2019 [cited 2019 Jun 6]. 176 p.
489 Available from: <http://www.sapea.info/topics/microplastics/report.pdf>
- 490 2. GESAMP. Sources, fate and effects of microplastics in the marine environment: a global
491 assessment. Kershaw P, editor. GESAMP (Group of Experts on the Scientific Aspects of Marine
492 Environmental Protection); 2015. 96 p. (GESAMP Reports & Studies Series).
- 493 3. UN Environment Programme. The State of Plastics [Internet]. 2018 Jun [cited 2021 Mar 26] p.
494 20. Available from: [https://www.unep.org/resources/report/state-plastics-world-environment-
495 day-outlook-2018](https://www.unep.org/resources/report/state-plastics-world-environment-day-outlook-2018)
- 496 4. Geyer R, Jambeck JR, Law KL. Production, use, and fate of all plastics ever made. *Science
497 Advances*. 2017 Jul;3(7):e1700782.
- 498 5. Alimi OS, Farner Budarz J, Hernandez LM, Tufenkji N. Microplastics and Nanoplastics in Aquatic
499 Environments: Aggregation, Deposition, and Enhanced Contaminant Transport. *Environmental
500 Science & Technology*. 2018 Feb 20;52(4):1704–24.
- 501 6. Horton AA, Walton A, Spurgeon DJ, Lahive E, Svendsen C. Microplastics in freshwater and
502 terrestrial environments: Evaluating the current understanding to identify the knowledge gaps
503 and future research priorities. *Science of The Total Environment*. 2017 May;586:127–41.
- 504 7. Lusher AL, Tirelli V, O'Connor I, Officer R. Microplastics in Arctic polar waters: the first reported
505 values of particles in surface and sub-surface samples. *Scientific Reports*. 2015 Oct
506 8;5(1):14947.
- 507 8. Obbard RW, Sadri S, Wong YQ, Khitun AA, Baker I, Thompson RC. Global warming releases
508 microplastic legacy frozen in Arctic Sea ice. *Earth's Future*. 2014 Jun;2(6):315–20.
- 509 9. Peeken I, Primpke S, Beyer B, Gütermann J, Katlein C, Krumpfen T, et al. Arctic sea ice is an
510 important temporal sink and means of transport for microplastic. *Nature Communications*
511 [Internet]. 2018 Dec [cited 2019 Jan 11];9(1). Available from:
512 <http://www.nature.com/articles/s41467-018-03825-5>
- 513 10. Yakushev E, Gebruk A, Osadchiv A, Pakhomova S, Lusher A, Berezina A, et al. Microplastics
514 distribution in the Eurasian Arctic is affected by Atlantic waters and Siberian rivers. *Commun
515 Earth Environ*. 2021 Dec;2(1):23.
- 516 11. Amélineau F, Bonnet D, Heitz O, Mortreux V, Harding AMA, Karnovsky N, et al. Microplastic
517 pollution in the Greenland Sea: Background levels and selective contamination of planktivorous
518 diving seabirds. *Environmental Pollution*. 2016 Dec;219:1131–9.
- 519 12. Morgana S, Ghigliotti L, Estévez-Calvar N, Stifanese R, Wieckzorek A, Doyle T, et al.
520 Microplastics in the Arctic: A case study with sub-surface water and fish samples off Northeast
521 Greenland. *Environmental Pollution*. 2018 Nov;242:1078–86.
- 522 13. Bergmann M, Wirzberger V, Krumpfen T, Lorenz C, Primpke S, Tekman MB, et al. High Quantities
523 of Microplastic in Arctic Deep-Sea Sediments from the HAUSGARTEN Observatory. *Environ Sci
524 Technol*. 2017 Oct 3;51(19):11000–10.
- 525 14. Tekman MB, Wekerle C, Lorenz C, Primpke S, Hasemann C, Gerdt G, et al. Tying up Loose Ends
526 of Microplastic Pollution in the Arctic: Distribution from the Sea Surface through the Water
527 Column to Deep-Sea Sediments at the HAUSGARTEN Observatory. *Environ Sci Technol*. 2020
528 Apr 7;54(7):4079–90.

- 1
2
3 529 15. Kim S-K, Lee H-J, Kim J-S, Kang S-H, Yang E-J, Cho K-H, et al. Importance of Seasonal Sea Ice in
4 530 the Western Arctic Ocean to the Arctic and Global Microplastic Budgets. *Journal of Hazardous*
5 531 *Materials*. 2021 May 8;125971. View Article Online
DOI: 10.1039/D1EM00280E
- 6 532 16. Kanhai LDK, Gårdfeldt K, Lyashevskaya O, Hassellöv M, Thompson RC, O'Connor I. Microplastics in
7 533 sub-surface waters of the Arctic Central Basin. *Marine Pollution Bulletin*. 2018 May;130:8–18.
- 8 534 17. Mu J, Zhang S, Qu L, Jin F, Fang C, Ma X, et al. Microplastics abundance and characteristics in
9 535 surface waters from the Northwest Pacific, the Bering Sea, and the Chukchi Sea. *Marine*
10 536 *Pollution Bulletin*. 2019 Jun;143:58–65.
- 11 537 18. Ross PS, Chastain S, Vassilenko E, Etemadifar A, Zimmermann S, Quesnel S-A, et al. Pervasive
12 538 distribution of polyester fibres in the Arctic Ocean is driven by Atlantic inputs. *Nat Commun*.
13 539 2021 Dec;12(1):106.
- 14 540 19. Kanhai LDK, Gardfeldt K, Krumpal T, Thompson RC, O'Connor I. Microplastics in sea ice and
15 541 seawater beneath ice floes from the Arctic Ocean. *Sci Rep*. 2020 Dec;10(1):5004.
- 16 542 20. Cózar A, Martí E, Duarte CM, García-de-Lomas J, van Sebille E, Ballatore TJ, et al. The Arctic
17 543 Ocean as a dead end for floating plastics in the North Atlantic branch of the Thermohaline
18 544 Circulation. *Sci Adv*. 2017 Apr 1;3(4):e1600582.
- 19 545 21. Obbard RW. Microplastics in Polar Regions: The Role of Long Range Transport. *Curr Opin*
20 546 *Environ Sci Health*. 2018;1:24–9.
- 21 547 22. van Sebille E, England MH, Froyland G. Origin, dynamics and evolution of ocean garbage
22 548 patches from observed surface drifters. *Environ Res Lett*. 2012 Dec 1;7(4):044040.
- 23 549 23. Kelly A, Lannuzel D, Rodemann T, Meiners KM, Auman HJ. Microplastic contamination in east
24 550 Antarctic sea ice. *Marine Pollution Bulletin*. 2020 May;154:111130.
- 25 551 24. Popova EE, Yool A, Coward AC, Dupont F, Deal C, Elliott S, et al. What controls primary
26 552 production in the Arctic Ocean? Results from an intercomparison of five general circulation
27 553 models with biogeochemistry. *Journal of Geophysical Research: Oceans* [Internet]. 2012 [cited
28 554 2021 Mar 3];117(C8). Available from:
29 555 <https://agupubs.onlinelibrary.wiley.com/doi/abs/10.1029/2011JC007112>
- 30 556 25. Thomas DN, Dieckmann G. *Sea ice: an introduction to its physics, chemistry, biology, and*
31 557 *geology*. Oxford, UK ; Malden, MA, USA: Blackwell Science; 2003. 402 p.
- 32 558 26. Stroeve J, Notz D. Changing state of Arctic sea ice across all seasons. *Environ Res Lett*. 2018
33 559 Sep;13(10):103001.
- 34 560 27. Fang C, Zheng R, Hong F, Jiang Y, Chen J, Lin H, et al. Microplastics in three typical benthic
35 561 species from the Arctic: Occurrence, characteristics, sources, and environmental implications.
36 562 *Environ Res*. 2021 Jan;192:110326.
- 37 563 28. Fang C, Zheng R, Zhang Y, Hong F, Mu J, Chen M, et al. Microplastic contamination in benthic
38 564 organisms from the Arctic and sub-Arctic regions. *Chemosphere*. 2018 Oct;209:298–306.
- 39 565 29. Gigault J, Halle A ter, Baudrimont M, Pascal P-Y, Gauffre F, Phi T-L, et al. Current opinion: What
40 566 is a nanoplastic? *Environmental Pollution*. 2018 Apr;235:1030–4.
- 41 567 30. van Sebille E, Wilcox C, Lebreton L, Maximenko N, Hardesty BD, van Franeker JA, et al. A global
42 568 inventory of small floating plastic debris. *Environmental Research Letters*. 2015 Dec
43 569 1;10(12):124006.
- 44 570 31. Eriksen M, Lebreton LCM, Carson HS, Thiel M, Moore CJ, Borerro JC, et al. Plastic Pollution in
45 571 the World's Oceans: More than 5 Trillion Plastic Pieces Weighing over 250,000 Tons Afloat at
46 572 Sea. Dam HG, editor. *PLoS ONE*. 2014 Dec 10;9(12):e111913.
- 47 573 32. Burns EE, Boxall ABA. Microplastics in the aquatic environment: Evidence for or against adverse
48 574 impacts and major knowledge gaps: Microplastics in the environment. *Environmental*
49 575 *Toxicology and Chemistry* [Internet]. 2018 Oct 16 [cited 2018 Oct 24]; Available from:
50 576 <http://doi.wiley.com/10.1002/etc.4268>
- 51 577 33. da Costa JP, Santos PSM, Duarte AC, Rocha-Santos T. (Nano)plastics in the environment –
52 578 Sources, fates and effects. *Science of The Total Environment*. 2016 Oct;566–567:15–26.
- 53 579 34. Gigault J, Pedrono B, Maxit B, Ter Halle A. Marine plastic litter: The unanalyzed nano-fraction.
54 580 *Environmental Science: Nano*. 2016;3(2):346–50.

- 1
2
3 581 35. Chamas A, Moon H, Zheng J, Qiu Y, Tabassum T, Jang JH, et al. Degradation Rates of Plastics in
4 582 the Environment. *ACS Sustainable Chem Eng.* 2020 Feb 27;acsuschemeng.9b06635. Article Online
DOI: 10.1039/D1EM00280E
- 5 583 36. Efimova I, Bagaeva M, Bagaev A, Kileso A, Chubarenko IP. Secondary Microplastics Generation
6 584 in the Sea Swash Zone With Coarse Bottom Sediments: Laboratory Experiments. *Front Mar Sci.*
7 585 2018 Sep 5;5:313.
- 8 586 37. El Hadri H, Gigault J, Maxit B, Grassl B, Reynaud S. Nanoplastic from Mechanically Degraded
9 587 Primary and Secondary Microplastics for Environmental Assessments. *NanoImpact.*
10 588 2020;17:100206.
- 11 589 38. Rochman CM, Browne MA, Underwood AJ, van Franeker JA, Thompson RC, Amaral-Zettler LA.
12 590 The ecological impacts of marine debris: unraveling the demonstrated evidence from what is
13 591 perceived. *Ecology.* 2016 Feb;97(2):302–12.
- 14 592 39. Allan J, Sokull-Kluettgen B, Patri A. Global Summit on Regulatory Science 2019 Nanotechnology
15 593 and Nanoplastics [Internet]. Publications Office of the European Union; 2020 [cited 2020 Oct 5].
16 594 Available from: <https://data.europa.eu/doi/10.2760/517689>
- 17 595 40. Wagner S, Reemtsma T. Things we know and don't know about nanoplastic in the environment.
18 596 *Nature Nanotechnology.* 2019 Apr;14(4):300–1.
- 19 597 41. Gigault J, El Hadri H, Nguyen B, Grassl B, Roweczyk L, Tufenkji N, et al. Nanoplastics are neither
20 598 microplastics norengineered nanoparticles. *Nature Nanotechnology.* 2021;In press.
- 21 599 42. Rowlands E, Galloway T, Manno C. A Polar outlook: Potential interactions of micro- and nano-
22 600 plastic with other anthropogenic stressors. *Science of The Total Environment.* 2021
23 601 Feb;754:142379.
- 24 602 43. Dumont I, Schoemann V, Lannuzel D, Chou L, Tison J-L, Becquevort S. Distribution and
25 603 characterization of dissolved and particulate organic matter in Antarctic pack ice. *Polar Biol.*
26 604 2009 May;32(5):733–50.
- 27 605 44. Eicken H. From the Microscopic, to the Macroscopic, to the Regional Scale: Growth,
28 606 Microstructure and Properties of Sea Ice. In: Thomas DN, Dieckmann GS, editors. *Sea Ice*
29 607 [Internet]. Oxford, UK: Blackwell Science Ltd; 2003 [cited 2021 Jun 11]. p. 22–81. Available
30 608 from: <http://doi.wiley.com/10.1002/9780470757161.ch2>
- 31 609 45. Aagaard K, Coachman LK, Carmack E. On the halocline of the Arctic Ocean. *Deep Sea Research*
32 610 *Part A Oceanographic Research Papers.* 1981 Jun;28(6):529–45.
- 33 611 46. Worster MG, Jones DWR. Sea-ice thermodynamics and brine drainage. Vol. 373, *Philosophical*
34 612 *Transactions of the Royal Society A: Mathematical, Physical and Engineering Sciences.* 2015. p.
35 613 20140166.
- 36 614 47. Lake RA, Lewis EL. Salt rejection by sea ice during growth. *J Geophys Res.* 1970 Jan
37 615 20;75(3):583–97.
- 38 616 48. Reimnitz E, Clayton JR, Kempema EW, Payne JR, Weber WS. Interaction of rising frazil with
39 617 suspended particles: tank experiments with applications to nature. *Cold Regions Science and*
40 618 *Technology.* 1993;21(2):117–35.
- 41 619 49. Nürnberg D, Wollenburg I, Dethleff D, Eicken H, Kassens H, Letzig T, et al. Sediments in Arctic
42 620 sea ice: Implications for entrainment, transport and release. *Marine Geology.* 1994 Jul;119(3–
43 621 4):185–214.
- 44 622 50. Ito M, Ohshima KI, Fukamachi Y, Hirano D, Mahoney AR, Jones J, et al. Favorable Conditions for
45 623 Suspension Freezing in an Arctic Coastal Polynya. *J Geophys Res Oceans.* 2019
46 624 Dec;124(12):8701–19.
- 47 625 51. Janssens J, Meiners KM, Tison J-L, Dieckmann G, Delille B, Lannuzel D. Incorporation of iron and
48 626 organic matter into young Antarctic sea ice during its initial growth stages. *Elem Sci Anth.* 2016
49 627 Aug 18;4(0):000123.
- 50 628 52. Bronstein VL, Itkin YA, Ishkov GS. Rejection and capture of cells by ice crystals on freezing
51 629 aqueous solutions. *Journal of Crystal Growth.* 1981 Apr;52:345–9.
- 52 630 53. Yemmou M, Briere A, Azouni MA. Rejection and capture of solid particles by ice. *Advances in*
53 631 *Space Research.* 1991 Jan;11(7):327–30.

- 1
2
3 632 54. Grossmann S, Gleitz M. Microbial responses to experimental sea-ice formation: Implications for the establishment of Antarctic sea-ice communities. *Journal of Experimental Marine Biology and Ecology*. 1993 Nov;173(2):273–89. Key Article Online
DOI: 10.1039/D1EM00280E
- 4 633
- 5 634
- 6 635 55. Hullar T, Anastasio C. Direct visualization of solute locations in laboratory ice samples. *The Cryosphere*. 2016 Sep 14;10(5):2057–68.
- 7 636
- 8 637 56. Kao JCT, Golovin AA, Davis SH. Particle capture in binary solidification. *J Fluid Mech*. 2009 Apr 25;625:299–320.
- 9 638
- 10 639 57. Geilfus N-X, Munson KM, Sousa J, Germanov Y, Bhugaloo S, Babb D, et al. Distribution and impacts of microplastic incorporation within sea ice. *Marine Pollution Bulletin*. 2019 Aug;145:463–73.
- 11 640
- 12 641
- 13 642 58. Lenz R, Enders K, Nielsen TG. Microplastic exposure studies should be environmentally realistic. *Proceedings of the National Academy of Sciences*. 2016 Jul 19;113(29):E4121–2.
- 14 643
- 15 644 59. Boyer TP, Baranova OK, Biddle M, Johnson DR, Mishonov AV, Paver C, et al. Arctic Regional Climatology, Regional Climatology Team, NOAA/NODC. 2012; Available from: http://www.nodc.noaa.gov/OC5/regional_climate/arctic/
- 16 645
- 17 646
- 18 647 60. Crabeck O, Galley R, Delille B, Else B, Geilfus N-X, Lemes M, et al. Imaging air volume fraction in sea ice using non-destructive X-ray tomography. *The Cryosphere*. 2016;10(3):1125–45.
- 19 648
- 20 649 61. Hare AA, Wang F, Barber D, Geilfus N-X, Galley RJ, Rysgaard S. pH evolution in sea ice grown at an outdoor experimental facility. *Marine Chemistry*. 2013 Aug;154:46–54.
- 21 650
- 22 651 62. Kowalik Z, Matthews JB. Numerical study of the water movement driven by brine rejection from nearshore Arctic ice. *Journal of Geophysical Research: Oceans*. 1983 Mar 30;88(C5):2953–8.
- 23 652
- 24 653
- 25 654 63. Thomas DN, Papadimitriou S, Michel C. Biogeochemistry of sea ice. In: *Sea ice* [Internet]. John Wiley & Sons, Ltd; 2009. p. 425–67. Available from: <https://onlinelibrary.wiley.com/doi/abs/10.1002/9781444317145.ch12>
- 26 655
- 27 656
- 28 657 64. Flemming H-C, Wingender J. The biofilm matrix. *Nat Rev Microbiol*. 2010 Sep;8(9):623–33.
- 29 658
- 30 659 65. Krembs C, Eicken H, Junge K, Deming JW. High concentrations of exopolymeric substances in Arctic winter sea ice: implications for the polar ocean carbon cycle and cryoprotection of diatoms. *Deep Sea Research Part I: Oceanographic Research Papers*. 2002 Dec 1;49(12):2163–81.
- 31 660
- 32 661
- 33 662 66. Pradel A, Ferreres S, Veclin C, El Hadri H, Gautier M, Grassl B, et al. Stabilization of Fragmental Polystyrene Nanoplastic by Natural Organic Matter: Insight into Mechanisms. *ACS EST Water* [Internet]. 2021 Mar 26 [cited 2021 Apr 11]; Available from: <https://doi.org/10.1021/acsestwater.0c00283>
- 34 663
- 35 664
- 36 665
- 37 666 67. Deville S. Freeze-Casting of Porous Ceramics: A Review of Current Achievements and Issues. *Adv Eng Mater*. 2008 Mar;10(3):155–69.
- 38 667
- 39 668 68. Alimi OS, Farner JM, Tufenkji N. Exposure of nanoplastics to freeze-thaw leads to aggregation and reduced transport in model groundwater environments. *Water Research*. 2021 Feb;189:116533.
- 40 669
- 41 670
- 42 671 69. Barb WG, Mikucki W. On the coagulation of polymer latices by freezing and thawing. *Journal of Polymer Science*. 1959;37(132):499–514.
- 43 672
- 44 673 70. Chou K-S, Liu H-L, Kao L-H, Yang C-M, Huang S-H. A quick and simple method to test silica colloids' ability to resist aggregation. *Colloids and Surfaces A: Physicochemical and Engineering Aspects*. 2014 Apr;448:115–8.
- 45 674
- 46 675
- 47 676 71. Benner R. Chapter 3 - Chemical Composition and Reactivity. In: Hansell DA, Carlson CA, editors. *Biogeochemistry of Marine Dissolved Organic Matter* [Internet]. San Diego: Academic Press; 2002. p. 59–90. Available from: <https://www.sciencedirect.com/science/article/pii/B9780123238412500051>
- 48 677
- 49 678
- 50 679
- 51 680 72. Giannelli V, Thomas DN, Haas C, Kattner G, Kennedy H, Dieckmann GS. Behaviour of dissolved organic matter and inorganic nutrients during experimental sea-ice formation. *Ann Glaciol*. 2001;33:317–21.
- 52 681
- 53 682
- 54
- 55
- 56
- 57
- 58
- 59
- 60

- 1
2
3 683 73. Xu R. Particle Characterization: Light Scattering Methods [Internet]. Springer Netherlands; View Article Online
4 684 2006. Available from: <https://books.google.fr/books?id=Y-HIBwAAQBAJ> DOI: 10.1039/D1EM00280E
5 685 74. Baalousha M, Lead JR. Rationalizing Nanomaterial Sizes Measured by Atomic Force Microscopy,
6 686 Flow Field-Flow Fractionation, and Dynamic Light Scattering: Sample Preparation,
7 687 Polydispersity, and Particle Structure. *Environ Sci Technol*. 2012 Jun 5;46(11):6134–42.
8 688 75. Asthana R, Tewari SN. The engulfment of foreign particles by a freezing interface. *JOURNAL OF*
9 689 *MATERIALS SCIENCE*. 1993 Oct;28(20):5414–25.
10 690 76. Körber C. Phenomena at the advancing ice–liquid interface: solutes, particles and biological
11 691 cells. *Quart Rev Biophys*. 1988 May;21(2):229–98.
12 692 77. Anderson ZT, Cundy AB, Croudace IW, Warwick PE, Celis-Hernandez O, Stead JL. A rapid
13 693 method for assessing the accumulation of microplastics in the sea surface microlayer (SML) of
14 694 estuarine systems. *Sci Rep*. 2018 Dec;8(1):9428.
15 695 78. Song YK, Hong SH, Jang M, Kang J-H, Kwon OY, Han GM, et al. Large Accumulation of Micro-
16 696 sized Synthetic Polymer Particles in the Sea Surface Microlayer. *Environ Sci Technol*. 2014 Aug
17 697 19;48(16):9014–21.
18 698 79. Tyagi S, Monteux C, Deville S. Multiple objects interacting with a solidification front. *Sci Rep*.
19 699 2021 Dec;11(1):3513.
20 700 80. Mountford AS, Morales Maqueda MA. Modeling the Accumulation and Transport of
21 701 Microplastics by Sea Ice. *J Geophys Res Oceans* [Internet]. 2021 Feb [cited 2021 Apr 15];126(2).
22 702 Available from: <https://onlinelibrary.wiley.com/doi/10.1029/2020JC016826>
23
24
25
26
27
28
29
30
31
32
33
34
35
36
37
38
39
40
41
42
43
44
45
46
47
48
49
50
51
52
53
54
55
56
57
58
59
60